PHYSICAL REVIEW B **84**, 100407(R) (2011)

Direct in-depth determination of a complex magnetic configuration in an exchange-coupled bilayer with perpendicular and in-plane anisotropy

J.-M. Tonnerre,[1,*] M. Przybylski,[2,3,†] M. Ragheb,[1] F. Yildiz,[2] H. C. N. Tolentino,[1] L. Ortega,[1] and J. Kirschner[2]

[1]*Institut Néel, CNRS and Université Joseph Fourier, BP166, F-38042 Grenoble Cedex 9, France*

[2]*Max-Planck-Institut für Mikrostrukturphysik, Weinberg 2, D-06120 Halle, Germany*

[3]*Faculty of Physics and Applied Computer Science, AGH University of Science and Technology, al. Mickiewicza 30, 30-059 Kraków, Poland*

(Received 20 April 2011; revised manuscript received 22 July 2011; published 26 September 2011)

By means of soft x-ray resonant magnetic reflectivity, we show that the utilization of different acquisition modes allows the separate analysis of in- and out-of-plane components of a complex magnetic configuration. This technique reveals high sensitivity towards magnetic inhomogeneity, in particular at interfaces. We found that Fe moments (in the layer with in-plane anisotropy) can be locally antiferromagnetically coupled to the layer of perpendicular anisotropy, when the layers are ferromagnetically exchange coupled.

DOI: 10.1103/PhysRevB.84.100407 PACS number(s): 75.30.Gw, 61.05.cm, 75.25.−j, 75.70.Cn

The competition between interlayer exchange coupling (IEC) and magnetic anisotropy of coupled films may result in a nonorthogonal magnetization configuration.[1] Such structures are important for magnetic recording and sensor technology.[2] Magnetometric techniques, as well as magneto-optic Kerr effect (MOKE) measurements, result in complex hysteresis loops for such a system.[1] However, a detailed (i.e., layer resolved) picture of the magnetic configuration cannot be determined from the hysteresis loops.

X-ray resonant magnetic reflectivity overcomes this limitation, since it allows an in-depth analysis of magnetic spin structures with a subnanometer scale spatial resolution. Typically, this technique is performed by analyzing the energy dependence of the reflectivity at different angular or scattering vector values,[3–8] whereas recently strong interest has emerged in the analysis of the angular dependence of the reflectivity close to an absorption edge.[9–13] This turns out to be particularly relevant in the soft x-ray range where the reflectivity measured at large scattering angles is sensitive to out-of-plane magnetization.[14] Recently, soft x-ray resonant magnetic reflectivity (SXRMR) has been used to resolve the in-depth magnetic structure with in-plane and perpendicular components.[15]

In this Rapid Communication, we show that by using circularly polarized light and different acquisition modes it is possible to separately analyze the in- and out-of-plane components of a complex magnetic configuration along the growth axis. It is particularly useful when the orientation of the magnetic moments are departing either from the easy axis of magnetization and/or from the direction of an external magnetic field.

Two kinds of magnetic bilayers exhibiting IEC were examined: $Rh_{cap}/Fe_{0.5}Co_{0.5}/Rh_{sp}(t)/Fe_{0.5}Co_{0.5}$, with $t = 7$ monolayers (ML) (sample S1) or $t = 3$ ML (sample S2), and $Rh_{cap}/Fe/Rh_{sp}(7\ ML)/Fe_{0.5}Co_{0.5}$ (sample S3). The samples were grown on Rh(001) at room temperature (RT) by molecular beam epitaxy.[16] The bottom $Fe_{0.5}Co_{0.5}$ layer is 8 ML thick for all three samples, and shows as a single layer an easy magnetization axis perpendicular to the sample plane.[16–18] The top $Fe_{0.5}Co_{0.5}$ layers in S1 and S2 are 6 ML thick and also show a perpendicular easy magnetization axis, whereas the top Fe layer in sample S3 is 6 ML thick and as a single layer shows ferromagnetic order below RT with an in-plane easy magnetization axis. The Rh spacer is known to mediate an exchange coupling, which can orient the magnetization either parallel or antiparallel, depending on the spacer thickness.[1] For S1 and S3 the coupling is expected to be ferromagnetic (FM), while for S2 it is expected to be antiferromagnetic (AF). The schematics of the S1 and S3 samples are shown in Fig. 1.

The samples were measured by polar MOKE at RT. Because of the loops (not shown here) we can assume that 6 ML of $Fe_{0.5}Co_{0.5}$ (S1) are ferromagnetic at RT and clearly contribute to the total polar Kerr signal, whereas 6 ML of Fe (S3) do not contribute to the polar Kerr signal. As a result, the polar saturation signal for S1 is almost double the saturation magnetization signal for S3, which proves that both $Fe_{0.5}Co_{0.5}$ layers have a perpendicular easy magnetization axis. An s-shaped loop, saturated at a relatively low field, is measured for S3 in longitudinal geometry. This indicates that T_c of 6 ML of Fe on Rh(001) is very close to RT and that the Fe film would be easiest magnetized in the sample plane. From the hysteresis loops measured at RT for S3 it is impossible to derive any conclusion on any complex magnetization configuration.

In order to gain more insight into the magnetic configuration of the perpendicular IEC bilayer systems, SXRMR experiments were carried out. The reflectivity is collected over a large angular range to fully benefit from the geometrical dependence of the energy-dependent atomic scattering factor.[14] The measurements were conducted at the SIM beamline[19] of the Swiss Light Source at the Paul Scherrer Institut (PSI), using circularly polarized light and the RESOXS end station[20] in the vicinity of the L_3 edge of Fe (706.8 eV). In order to probe the perpendicular magnetization component (m_z), the measurements were performed in polar geometry, where the sample is magnetized by a permanent perpendicular magnet of $\mu_0 H = 0.4$ T brought to the sample surface, followed by data collection in remanence.[14] In this case, the reflectivity I_p and I_m were obtained by reversing the x-ray helicity, which is equivalent to reversing the orientation of the net magnetization in each layer (so-called acquisition mode A). The measurements for probing m_y were also performed in longitudinal geometry using an electromagnet for sample

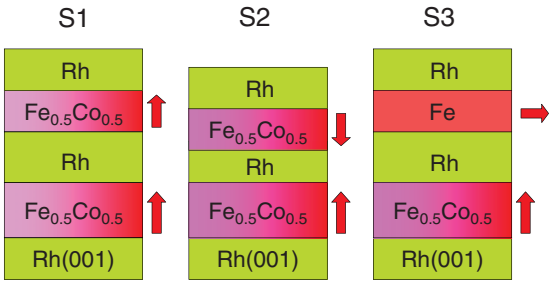

FIG. 1. (Color online) Schematic of the S1, S2, and S3 samples.

magnetization.[20] I_p and I_m were obtained by reversing a longitudinally applied magnetic field ($\mu_0 H$ up to 0.16 T) while keeping the x-ray helicity unchanged (mode B). Here, only the in-plane magnetization component is expected to flip.

The quantitative analysis of SXRMR aims at determining the magnetic profile along the growth axis. The structural parameters are derived from the refinement of x-ray reflectivity curves measured at RT far from the edge (including a Cu $K\alpha$ x-ray source) and near the Fe and Co L edges, taking advantage of the specific charge contrast introduced at the resonance. The magnetic profile is derived from the refinement of the magnetic asymmetry $R = (I_p - I_m)/(I_p + I_m)$, while keeping the structure parameters constant. The magnetic film can be subdivided into slices. The magnetization vector of each slice can be described by an amplitude term and two angles. The magnetic amplitude of each slice is refined by adjusting a weighting factor w_m that modifies the amplitude of the magnetic resonant terms. The Fe charge and magnetic resonant terms used in the energy-dependent refraction index, or atomic scattering factor,[21] are obtained from x-ray magnetic circular dichroism (XMCD) data for a thick Fe film.[22] Although the Fe in the $Fe_{0.5}Co_{0.5}$ layers exhibits a strained structure ($c/a = 1.2$) leading to a higher m_L/m_S ratio,[17] the use of the thick-Fe reference system is believed to be suitable since it is evaluated from a direct comparison of the shape of the absorption spectrum and of the XMCD signal at the Fe L edge.[22] Also, we cannot exclude the effect of a slightly different energy resolution on the scattering amplitude. However, since we analyze the angle-dependent reflectivity at specific energies rather than energy-dependent reflectivity at various angles, the possible error in the absolute amplitude (estimated to be in the range of 15%) is not expected to remarkably modify the magnetic profile. A value of $w_m = 1$ corresponds to $2.1\mu_B$. The simulations are performed using the Zaḱs approach[23] and taking into account the interfacial roughness issue.[24]

We first investigated the magnetic configuration in the S1 sample. Figure 2(a) shows I_p and I_m measured in acquisition mode A at RT at 705.2 eV, close to the first inflexion point of the Fe L_3 edge, optimizing the intensity of the real part while keeping the absorption low. The refined thickness and roughness parameters for each layer of S1 are (in nm) 2.08(5), 0.29(7)/1.05(7), 0.26(9)/1.19(4), 0.23(7)/1.31(5), 0.17(8). Figure 2(b) shows the analysis of the magnetic asymmetry. The lack of asymmetry at small angles is in agreement with a pure net out-of-plane magnetization.[13,15] The dashed (blue) line displays the calculated asymmetry by considering a homogeneous perpendicular Fe magnetization

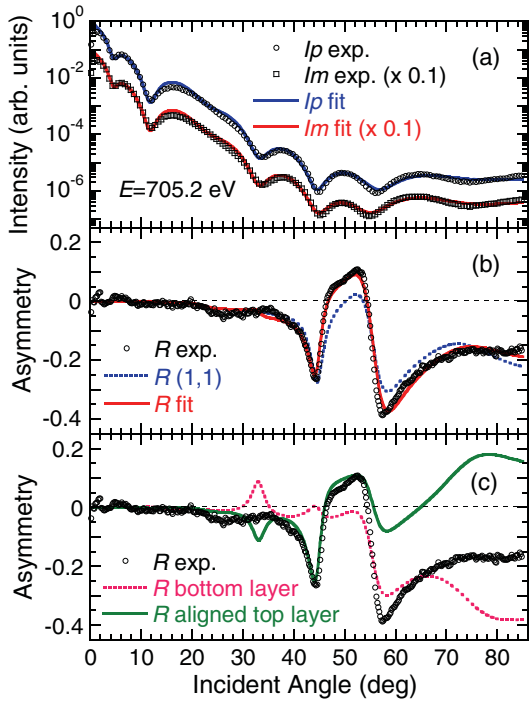

FIG. 2. (Color online) (a) Reflectivity and (b) magnetic asymmetry measured in mode A for sample S1. $R(1,1)$ denotes the calculated asymmetry by considering homogeneous magnetization for both ferromagnetically coupled $Fe_{0.5}Co_{0.5}$ layers, R-fit denotes the best fit obtained after allowing inhomogeneity in the magnetic amplitude throughout both layers. (c) Magnetic asymmetry from the best fit of (b) plotted separately for bottom and top $Fe_{0.5}Co_{0.5}$ layers.

($w_m = 1$) along the growth axis of both $Fe_{0.5}Co_{0.5}$ layers coupled ferromagnetically. The solid (red) line displays the fit of the data. Very good agreement is obtained by allowing inhomogeneity in the magnetic amplitude throughout both layers. Such good agreement is not achievable by considering the possibility of a net in-plane magnetic component, neither m_x nor m_y. After dividing the layers into three equally thick slices of 0.3–0.4 nm, a reduced magnetization (by 5%–20%) is observed at the interfaces, which is likely to be related to the changes in concentration due to intermixing and/or the lateral averaging of local thickness variations.[4] Figure 2(c) shows, together with the experimental data, the asymmetry when the magnetization only of the bottom layer [dashed (magenta) line] and only in the top layer [solid (green) line] is considered. We note that the first dip (at 44°) is related to the magnetization of the top layer parallel aligned with the magnetization of the bottom layer, which is responsible for the second dip (at 56°).

We turn to sample S2 to investigate the effect of AF coupling between both layers on R. Figure 3(a) exhibits I_p and I_m measured in acquisition mode A at RT, at 705.2 eV. The refined thickness and roughness parameters for each layer of S2 are (in nm) 2.08(9),0.31(7)/1.09(7),0.22(6)/0.43(7),0.23(9)/1.18(8),0.11(9), respectively. Figure 3(b) shows the analysis of the magnetic asymmetry. The dashed (blue) line displays the calculated asymmetry by considering a homogeneous perpendicular magnetization ($w_m = 1$) in both $Fe_{0.5}Co_{0.5}$

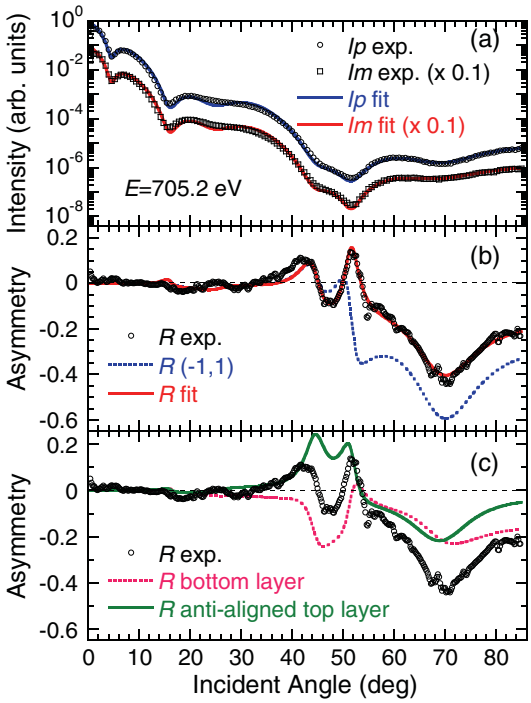

FIG. 3. (Color online) (a) Reflectivity and (b) magnetic asymmetry measured in mode A for sample S2. $R(-1,1)$ denotes the calculated asymmetry by considering homogeneous magnetization for both antiferromagnetically coupled $Fe_{0.5}Co_{0.5}$ layers, and R-fit denotes the best fit obtained after allowing inhomogeneity in the magnetic amplitude throughout both layers. (c) Magnetic asymmetry from the best fit of (b) plotted separately for bottom and top $Fe_{0.5}Co_{0.5}$ layers.

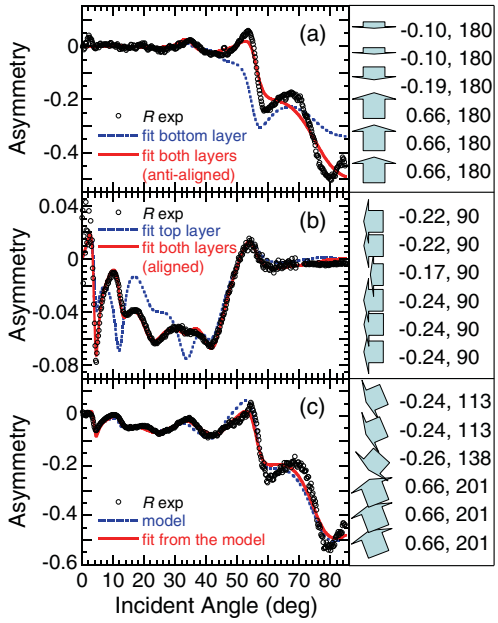

FIG. 4. (Color online) Left-hand panel: Asymmetry measured for sample S3 in mode A (a), in mode B (b), and in mode C (c) at 705.2 eV. Right-hand panel: Magnetic profile with weighting factors w_m and angles in the yz plane.

layers, with the top layer aligned antiparallel with the bottom one. Only the first feature of the experimental asymmetry at 43° is well reproduced. The solid (red) line displays the fit of the data. Again, very good agreement is obtained by allowing inhomogeneity in the magnetic amplitude throughout both layers. Especially the second positive feature in the asymmetry at 52° is particularly sensitive to reduction at interfaces. We note in Fig. 3(c) that the change of sign of the first feature, as well as the largest asymmetry at high angles, can be related to the opposite direction of the magnetization in the top layer [solid (green) line]. The difference in the shape of the asymmetry as compared to Fig. 2(c) is caused by the structural difference [see Figs. 2(a) and 3(a)]. Figures 2(c) and 3(c) show that the sign of the asymmetry of the first strong feature (at 44°) in the asymmetry can be an indication for the alignment (parallel or antiparallel) of the perpendicular components of the magnetization in the coupled layers.

We finally discuss sample S3, where a complex magnetic configuration can be produced since both magnetic layers exhibit a different magnetic anisotropy and a presence of IEC. We present the results obtained at RT. The refined thickness and roughness parameters for each layer of S3 are (in nm) 22.0(7),0.35(5)/1.03(6),0.28(5)/1.09(7),0.22(6)/1.36(6),0.21(6). In order to probe the out-of-plane magnetization, the measurements were performed in acquisition mode A. I_p and I_m are collected at 705.2 eV and the derived asymmetry is shown in Fig. 4(a). The amplitude of the signal is close to zero up to $\theta = 30°$ and increases at large angles. The first attempt to fit the asymmetry is performed by considering a perpendicular magnetic contribution only in the $Fe_{0.5}Co_{0.5}$ layer, because of its strong perpendicular anisotropy and no magnetic contribution from the top Fe layer [dashed (blue) line in Fig. 4(a)]. A homogeneous distribution inside the $Fe_{0.5}Co_{0.5}$ film leads to large discrepancies with the data. Taking into account the possibility of inhomogeneity inside the layer, as for S1 and S2, does not result in significant progress. This prompts us to consider the existence of an additional out-of-plane magnetic contribution in the 6-ML-thick Fe layer. Although paramagnetic at RT, it shows a residual net magnetization related to the coupling with the $Fe_{0.5}Co_{0.5}$ layer underneath. The best refinement [solid (red) line] reveals a contribution, opposite to the magnetization in the $Fe_{0.5}Co_{0.5}$ layer, twice as large in the slice at the bottom interface of the Fe layer than in the others. The values of the w_m parameters are given, together with the angular value corresponding to the perpendicular magnetization, next to Fig. 4(a). The contributions from the slices of the bottom $Fe_{0.5}Co_{0.5}$ layer are similar within 15% and the same value is reported. This low value (66% of the average w_m for S1 and S2) is ascribed to an improper magnetization of the sample by the permanent magnet during the experiment. Only a net antiparallel magnetization in the top Fe layer enables us to fit the positive feature of the asymmetry at 54°. This result is consistent with the analysis of the magnetic asymmetry for S1 and S2. The origin of this unexpected antiparallel alignment might be related to the actual local thickness of the separating Rh layer. Taking into account the fitted Rh_{sp} thickness of 1.09 nm, the Rh spacer turns out to be 5.7 ML thick rather than 7 ML. Hence, and due to the value of 0.22-nm rms roughness of the Rh interface, areas 4–5 and 6–7 ML thick could coexist. Thus, a mixture of thicknesses

leading to a different nature and strength of the IEC could be characteristic for this sample[1] and the AF coupling could be locally expected. Since the AF coupling is stronger than the FM one, it is not surprising that locally ferromagnetically ordered Fe moments, antiferromagnetically coupled to the bottom $Fe_{0.5}Co_{0.5}$ layer, contribute to the asymmetry signal probed in mode A.

The in-plane magnetization was probed using acquisition mode B. The hysteresis curve, recorded in specular reflectivity condition at an incident angle of 8°, shows an s-shaped loop with 4.6% variation, indicating the presence of a small net in-plane component. Such a contribution can originate from a net magnetization of Fe in the top Fe layer induced by the applied magnetic field and/or from the rotation of the perpendicular magnetization of the Fe atoms in the $Fe_{0.5}Co_{0.5}$ layer toward the field direction. Figure 4(b) shows the asymmetry resulting from the mode B measurement. It develops at small angles and is close to zero above $\theta = 60°$, in agreement with the absence of a perpendicular component. Indeed, the perpendicular component is not reversed and does not contribute to the asymmetry. The net in-plane magnetization component was initially considered only in the Fe layer [dashed (blue) line]. Because of the discrepancy, we have to take into account an in-plane magnetic contribution in the $Fe_{0.5}Co_{0.5}$ layer. The best refinement indicates that aligned in-plane magnetic components in both layers are required to fit the asymmetry [solid (red) line]. This shows that the magnetic moments in the $Fe_{0.5}Co_{0.5}$ layer are rotated to follow the applied magnetic field. The values of the w_m parameters are given in the table next to Fig. 4(b). The low magnetization value in the Fe layer is related to T_c, which is below RT. The high quality of the fit forces the amplitude of the magnetization in the bottom slice of the Fe layer to be 23% smaller than in the two other slices. This is attributed to the coupling effect proven in mode A, which does not affect the whole layer.

The measurements were also performed in a third mode called C. It corresponds to a mixture of mode A, where the circular polarized light is reversed, and of mode B, since a magnetic field is applied in one fixed direction. This magnetic field defines a preferential orientation for the Fe magnetic moments in the top Fe layer and possibly a rotation of those in the bottom $Fe_{0.5}Co_{0.5}$ layer. In this case, reversing the polarization is equivalent to reversing both the in-plane and out-of-plane magnetization components. This is clearly seen in Fig. 4(c), where the asymmetry exhibits both a signal at small angles and at large angles, corresponding to the in- and out-of-plane magnetization components, respectively. The asymmetry measured in mode C is only slightly different from the sum of the asymmetries acquired in the A and B modes. Indeed, in mode C the out-of-plane contribution corresponds to the projection of the magnetic moment along the z axis, whereas in mode A the out-of-plane contribution corresponds to the full amplitude of the magnetic moment.

The analysis of the asymmetries in modes A and B allows the building of a complex magnetic structure where the magnetic moments are described in the yz plane with different amplitudes and orientations for three different slices of each layer [table next to Fig. 4(c)]. In the Fe layer, the results of modes A and B are considered, in a first approach, as the z and y magnetization components in mode C. The reality may be slightly different, since the Fe layer in mode A does not feel the presence of an in-plane magnetic field. For the $Fe_{0.5}Co_{0.5}$ layer, the results of mode A provide the amplitude of the magnetization, and the results of mode B yield the projection of the magnetization to the y axis. The error bars for the angles are estimated to be $\sim 10°$ and 4° in the Fe and $Fe_{0.5}Co_{0.5}$ layers, respectively. The proposed model can very nicely reproduce the asymmetry measured in mode C [dashed (blue) line in Fig. 4(c)]. A further refinement, carried out by limiting the parameters within the estimated error bars, allows us to improve the agreement between the calculated and experimental asymmetries [solid (red) line]. An attempt to directly refine the asymmetry, at first considering only two parameters (amplitude and orientation) for each magnetic layer, does not allow a good fit. Nevertheless, it yields $(-0.34, 130°)$ for the Fe layer and $(0.68, 197°)$ for the $Fe_{0.5}Co_{0.5}$ layer, which is consistent with our findings. Any attempt to directly resolve the distribution of the amplitude and angles failed since it implies too many parameters.

In conclusion, we have shown that SXRMR can resolve complex magnetic configurations. In particular, we can probe the spatial distribution of both in-plane and perpendicular magnetization components along the growth axis in an IEC system with magnetic layers exhibiting alternated in-plane and perpendicular easy magnetization axis. We obtained a robust magnetic profile from using different configurations, being only sensitive to either the perpendicular component, or to the in-plane component, or to both. Furthermore, SXRMR reveals a high sensitivity toward magnetic inhomogeneity, especially at interfaces. This Rapid Communication shows how otherwise hidden details of the interaction between two magnetic films can be investigated. We expect this approach to allow the description of fine details in composite and magnetoelectric systems for which the understanding of the magnetic properties requires an understanding of the modifications induced at the interfaces.

*jean-marc.tonnerre@grenoble.cnrs.fr

†mprzybyl@mpi-halle.de

[1] F. Yildiz, M. Przybylski, and J. Kirschner, Phys. Rev. Lett. **103**, 147203 (2009).

[2] A. Taga, L. Nordström, P. James, B. Johansson, and O. Eriksson, Nature (London) **406**, 280 (2000).

[3] J. M. Tonnerre, L. Sève, D. Raoux, G. Soullié, B. Rodmacq, and P. Wolfers, Phys. Rev. Lett. **75**, 740 (1995).

[4] L. Sève, N. Jaouen, J. M. Tonnerre, D. Raoux, F. Bartolomé, M. Arend, W. Felsch, A. Rogalev, J. Goulon, C. Gautier, and J. F. Bérar, Phys. Rev. B **60**, 9662 (1999).

[5] M. Sacchi and C. F. Hague, Surf. Rev. Lett. **9**, 811 (2002).

[6] J. W. Freeland, K. E. Gray, L. Ozyuyer, P. Berghuis, E. Badica, J. Kavich, H. Zheng, and J. F. Mitchell, Nat. Mat. **4**, 62 (2005).

[7] A. Bergmann, J. Grabis, A. Nefedov, K. Westerholt, and H. Zabel, J. Phys. D **39**, 842 (2006).

[8]S. Valencia, A. Gaupp, W. Gudat, L. Abad, L. Balcells, and B. Martinez, J. App Phys. **104**, 023903 (2008).

[9]J. W. Freeland, V. Chakarian, Y. U. Idzerda, S. Doherty, J. G. Zhu, J.-H. Park, and C.-C. Kao, Appl. Phys. Lett. **71**, 276 (1997).

[10]Y. Choi, D. Haskel, R. E. Camley, D. R. Lee, J. C. Lang, G. Srajer, J. S. Jiang, and S. D. Bader, Phys. Rev. B **70**, 134420 (2004).

[11]K.-S. Lee, D.-E. Jeong, S.-K. Kim, and J. B. Kortright, J. Appl. Phys. **97**, 083519 (2005).

[12]S. Roy, M. R. Fitzsimmons, S. Park, M. Dorn, O. Petracic, Igor V. Roshchin, Zhi-Pan Li, X. Batlle, R. Morales, A. Misra, X. Zhang, K. Chesnel, J. B. Kortright, S. K. Sinha, and Ivan K. Schuller, Phys. Rev. Lett. **95**, 047201 (2005).

[13]S. Brück, G. Schütz, E. Goering, X. Ji, and K. M. Krishnan, Phys. Rev. Lett. **101**, 126402 (2008).

[14]J.-M. Tonnerre, M. De Santis, S. Grenier, H. C. N. Tolentino, V. Langlais, E. Bontempi, M. Garcia-Fernandez, and U. Staub, Phys. Rev. Lett. **100**, 157202 (2008).

[15]H. L. Meyerheim, J.-M. Tonnerre, L. Sandratskii, H. C. N. Tolentino, M. Przybylski, Y. Gabi, F. Yildiz, X. L. Fu, E. Bontempi, S. Grenier, and J. Kirschner, Phys. Rev. Lett. **103**, 267202 (2009).

[16]F. Yildiz, M. Przybylski, and J. Kirschner, J. Appl. Phys. **105**, 07C312 (2009).

[17]F. Yildiz, F. Luo, C. Tieg, R. M. Abrudan, X. L. Fu, A. Winkelmann, M. Przybylski, and J. Kirschner, Phys. Rev. Lett. **100**, 037205 (2008).

[18]F. Yildiz, M. Przybylski, X.-D. Ma, and J. Kirschner, Phys. Rev. B **80**, 064415 (2009).

[19]U. Flechsig, F. Nolting, A. Fraile-Rodriguez, J. Krempasky, C. Quitmann, T. Schmidt, S. Spielmann, and D. Zimoch, in *SRI 2009, 10th International Conference on Synchrotron Radiation Instrumentation*, edited by R. Garrett, I. Gentle, K. Nugent, and S. Wilkins, AIP Conf. Proc. Vol. 1234 (AIP, Melville, NY, 2010), p. 319.

[20]N. Jaouen, J.-M. Tonnerre, G. Kapoujian, P. Taunier, J.-P. Roux, D. Raoux, and F. Sirotti, J. Synchrotron Radiat. **11**, 353 (2004).

[21]J. B. Kortright and Sang-Koog Kim, Phys. Rev. B **62**, 12216 (2000).

[22]C. T. Chen, Y. U. Idzerda, H.-J. Lin, N. V. Smith, G. Meigs, E. Chaban, G. H. Ho, E. Pellegrin, and F. Sette, Phys. Rev. Lett. **75**, 152 (1995).

[23]J. Zak, E. R. Moog, C. Liu, and S. D. Bader, Phys. Rev. B **43**, 6423 (1991).

[24][http://dimgruppi.ing.unibs.it/chimica/Bontempi/Reftool/reftool.html].